describing effects of exposure of female mice and rats to very low doses of BPA during perinatal development on the mammary glands (Jenkins et al. 2009). Although Tyl et al. (2008a) reported no low-dose effects of BPA on the mammary glands using conventional histologic analysis, there have been consistent findings of adverse effects of low doses of BPA from studies that used more sophisticated and sensitive analysis of whole mounted mammary glands to facilitate detection of microscopic lesions, coupled with immunostaining for regulatory proteins as well as techniques for determination of aberrant gene expression associated with progression to cancer. These peer-reviewed studies have reported detecting changes during embryonic development of mammary glands as well as abnormalities detected during adolescence through adulthood that are indicative of mammary gland cancer as well as other developmental abnormalities (Colerangle and Roy 1997; Durando et al. 2007; Jenkins et al. 2009; LaPensee et al. 2008; Markey et al. 2001, 2005; Moral et al. 2008; Munoz-de-Toro et al. 2005; Murray et al. 2007; Nikaido et al. 2004; Vandenberg et al. 2006, 2007b; Wadia et al. 2007).

Similar to the findings for the mammary gland, Ogura et al. (2007) reported that if tissues were analyzed by conventional histologic methods (staining with hematoxalin and eosin), prenatal exposure to low doses of BPA or DES showed no effects on prostate development, whereas if the sections were analyzed using antibodies that identified basal cells and basal cell squamous metaplasia, then significant effects were revealed. Squamous metaplasia of basal cells indicates abnormal proliferation and function of the prostate stem cell population that is thought to transform into neoplastic cells; Ho et al. (2006) reported that neonatal exposure to very low doses of BPA caused 100% of male rats to develop high-grade prostatic intraepithelial neoplastic lesions later in life. All of these studies were rejected by the U.S. FDA as not adequate for making regulatory decisions about the safety of BPA. Instead, the U.S. FDA relied upon Tyl et al. (2008a), even though the study used techniques that Ogura et al. (2007) showed lacked the sensitivity of 21st century experimental approaches.

Although findings regarding changes in brain structure, brain chemistry, and behavior represent the largest portion of the literature on low-dose BPA, Tyl et al. (2008a) did not examine any neurobehavioral end points. The NTP (2008) and the NIEHS conference consensus reports (vom Saal et al. 2007) both indicated concern about neurobehavioral effects of low doses of BPA. Thus, the absence of studies that included neurobehavioral end points is a glaring omission of Tyl et al. (2008a, 2008b).

Flawed prostate dissection. Data presented by Tyl et al. (2008a) raise questions about the adequacy of techniques used in their BPA studies. Specifically, Tyl et al. (2008a) reported that the prostate in 3.5-month-old control male CD-1 mice weighed > 70 mg [see Table 3 in Tyl et al. (2008a) for data on F_1 retained males]. This average control weight contrasts sharply with those reported from other laboratories. Specifically, the weight of the prostate in 2- to 3-month-old CD-1 mice using the dissection technique based on both Ruhlen et al. (2008) and Gupta (2000) and at the NIEHS (Newbold RR, personal communication) is about 40 mg. Several studies have reported that prenatal exposure to very low doses of BPA and positive control estrogens increased prostate size, prostatic androgen receptors, and prostate androgen receptor gene activity (Gupta 2000; Richter et al. 2007b; Thayer et al. 2001; Timms et al. 2005; vom Saal et al. 1997), but the enlarged prostate of experimental animals exposed to BPA in these laboratories weighed less than the prostates in the control animals of Tyl et al. (2008a). This raises serious questions about the procedures and/or animals used by Tyl et al. The weight of prostate reported by Tyl et al. (2008a) suggests that the technique used for dissecting the prostate resulted in nonprostatic tissue being weighed along with prostate. The seminal vesicle, coagulating gland, and dorsolateral prostate all merge together where the ejaculatory ducts enter the urethra, and there are also fat deposits on the prostate. This poses a challenge for those without proper training in distinguishing these different tissues during dissection in mice.

Alternatively, as male rodents age, they are prone to develop prostatitis. Although this inflammatory disease leads to an increase in prostate size and could thus account for the very large prostate weights reported by Tyl et al. (2008a), anyone familiar with the appearance of prostatitis would detect this abnormality upon histologic examination, which Tyl et al (2008a) supposedly conducted. Also, prostatitis is rare in young-adult mice or rats (Cowin et al. 2008), and the size of the prostates in the Tyl et al. (2008a) study were similar to those for middle-aged and old male mice.

The findings regarding effects of BPA on the prostate presented by Tyl et al. (2008a) are thus suspect and cannot be used as evidence that other earlier studies (Gupta 2000; Timms et al. 2005; vom Saal et al. 1997) are not replicable. Given these problems in prostate weight measurements, it is not surprising that even very high doses of BPA or estradiol reported by Tyl et al. (2008a) had no effect on the prostate, in sharp contrast to other studies that showed stimulation of the prostate at low doses of estrogen and inhibition at high doses (Putz et al. 2001; Timms et al. 2005).

In addition to the problem associated with the high prostate weight reported by Tyl et al. (2008a), in a separate measurement the authors combined the anterior prostate (coagulating gland) and seminal vesicle, presenting these two organs as one combined outcome measure. This is wrong and misleading. The coagulating glands emerge as the anterior ducts of the prostate from the dorsocranial region of the urogenital sinus, whereas the seminal vesicles bud from the proximal region of the Wolffian ducts. Elevated estrogen is associated with an increase in prostate size associated with an increase in prostate androgen receptors, whereas a decrease in seminal vesicle size is associated with a reduction in 5α-reductase, an enzyme that converts testosterone to the more potent androgen 5α-dihydrotestosterone (Nonneman et al. 1992). Low doses of BPA have been shown to decrease the size of organs that differentiate from the embryonic Wolffian ducts (epididymides and seminal vesicles) while increasing the size of regions of the prostate that develop from the urogenital sinus (vom Saal et al. 1998). Combining these different organs (it is technically not difficult to separate them) was thus inappropriate because they develop from different embryonic tissues that show markedly different responses to estrogenic chemicals during development. In fact, Ogura et al. (2007) reported that the anterior prostate (coagulating glands) showed the greatest expression of ER-α, and also showed the most pronounced indication of basal cell squamous metaplasia in response to developmental exposure to low doses of DES and BPA relative to other regions of the prostate.

Conclusions

Because the control data of Tyl et al. (2008a) were not consistent with the prior published literature for prostate weight of young-adult CD-1 male mice and because their methods were inappropriate for revealing an extensive body of adverse effects detected using more sophisticated approaches, we deem the findings by Tyl et al. to be invalid. Hundreds of studies show adverse effects of BPA in animals, with many conducted at concentrations equivalent to current human levels of BPA exposure; thus, it is unlikely that academic scientists would bother to replicate the outdated approaches used by Tyl et al. (2008a, 2008b). This lack of replication is typical of GLP studies, which tend to involve unnecessarily large numbers of animals [Tyl et al. (2002) used > 8,000 rats], and reliability appears to be accepted because of the numbers of animals that were used. Although using excessive numbers of animals is accepted as good science by the U.S. FDA, the use of arbitrarily large numbers of animals per group (> 20 animals per treatment group is common) actually violates guidelines in the NIH *Guide for the*

Care and Use of Laboratory Animals (Institute of Laboratory Animal Research 1996) that govern research conducted by academic and government scientists. For research with animals to be approved by any university animal care and use committee, group sizes must be based on power analysis conducted using historic data. Based on this criterion in the NIH Guide, all of the studies by Tyl et al. were significantly over powered and thus in direct violation of federal guidelines for conducting animal research, a fact about which U.S. FDA regulators seem unaware.

Each of the four main industry-funded GLP studies of BPA (Ashby et al. 1999; Cagen et al. 1999; Tyl et al. 2008a, 2008b) is flawed and not appropriate for use in setting health standards. Clearly, meeting GLP standards is not a guarantee of reliable or valid science. It is of great concern that the U.S. and EU regulatory communities are willing to accept these industry-funded, antiquated, and flawed studies as proof of the safety of BPA while rejecting as invalid for regulatory purposes the findings from a very large number of academic and government investigators using 21st-century scientific approaches. The basis for these decisions by U.S. and EU regulatory agencies should be thoroughly investigated, particularly since the NTP (2008) concluded that BPA exposure to human infants was in the range shown to cause harm in experimental animals and since both the Canadian Ministry of Health and the Ministry of the Environment recently concluded that BPA was a toxic chemical (Environment Canada 2008).

Problems inherent with reliance on GLP as the standard for choosing data are compounded by the process used by federal agencies to determine membership on science advisory panels. Leading experts qualified by specific experience on the chemical or end points under consideration are often specifically excluded from membership. For example, the U.S. FDA's BPA review panel was identified as an expert panel, when in fact the panel was composed largely of scientists lacking any experience in research with BPA. This process, which appears to consider almost any scientist knowledgeable about a chemical to create bias, makes it vastly more difficult for the panel to integrate scientific data from the relevant literature, especially since, as with BPA, there are almost 1,000 relevant studies and the review panel is provided with very little time to become knowledgeable about the details. It means that the depth of knowledge present on this and similarly constituted government regulatory agency panels is unlikely to be sufficient to subject draft assessments to the scrutiny that peer review by experts normally entails. Combined with reliance on GLP data, this process has a high potential to yield flawed assessments that jeopardize public health.

We are not suggesting that GLP should be abandoned as a requirement for industry-funded studies. We object, however, to regulatory agencies implying that GLP indicates that industry-funded GLP research is somehow superior to NIH-funded studies that are not conducted using GLP. This argument demonstrates a lack of understanding of the profound difference between the use of replication as a mechanism to assess reliability and the methods used to assess validity for peer-reviewed published academic studies, whereas GLP was instituted with the expectation that this type of verification would not occur.

Public health decisions should be based on studies using appropriate protocols and the most sensitive assays. They should not be based on criteria that include or exclude data depending on whether or not the studies use GLP. Simply meeting GLP requirements is insufficient to guarantee scientific reliability and validity.

References

Alonso-Magdalena P, Laribi O, Ropero AB, Fuentes E, Ripoll C, Soria B, et al. 2005. Low doses of bisphenol A and diethylstilbestrol impair Ca^{2+} signals in pancreatic α cells through a nonclassical membrane estrogen receptor within intact islets of Langerhans. Environ Health Perspect 113:969–977.

Alonso-Magdalena P, Morimoto S, Ripoll C, Fuentes E, Nadal A. 2006. The estrogenic effect of bisphenol A disrupts pancreatic β-cell function *in vivo* and induces insulin resistance. Environ Health Perspect 114:106–112.

Alonso-Magdalena P, Ropero AB, Carrera MP, Cederroth CR, Baquie M, Gauthier BR, et al. 2008. Pancreatic insulin content regulation by the estrogen receptor ERα. PLoS ONE 3(4):e2069; doi:10.1371/journal.pone.0002069 [Online 30 April 2008].

Ashby J, Tinwell H, Haseman J. 1999. Lack of effects for low dose levels of bisphenol A (BPA) and diethylstilbestrol (DES) on the prostate gland of CF1 mice exposed in utero. Regul Toxicol Pharmacol 30:156–166.

Cagen SZ, Waechter JM, Dimond SS, Breslin WJ, Butala JH, Jekat FW, et al. 1999. Normal reproductive organ development in CF-1 mice following prenatal exposure to bisphenol A. Toxicol Sci 11:15–29.

CERHR (Center for the Evaluation of Risks to Human Reproduction). 2007. NTP-CERHR Expert Panel Report on the Reproductive and Developmental Toxicity of Bisphenol A. NTP-CERHR-BPA-07. Available: http://cerhr.niehs.nih.gov/chemicals/bisphenol/BPAFinalEPVF112607.pdf [accessed 28 July 2008].

Colerangle JB, Roy D. 1997. Profound effects of the weak environmental estrogen-like chemical bisphenol A on the growth of the mammary gland of Noble rats. J Steroid Biochem Mol Biol 60(1–2):153–160.

Cowin PA, Foster P, Pedersen J, Hedwards S, McPherson SJ, Risbridger GP. 2008. Early-onset endocrine disruptor-induced prostatitis in the rat. Environ Health Perspect 116:923–929.

Crain DA, Eriksen M, Iguchi T, Jobling S, Laufer H, LeBlanc GA, et al. 2007. An ecological assessment of bisphenol-A: evidence from comparative biology. Reprod Toxicol 24(2):225–239.

Durando M, Kass L, Piva J, Sonnenschein C, Soto AM, Luque EH, et al. 2007. Prenatal bisphenol A exposure induces preneoplastic lesions in the mammary gland in Wistar rats. Environ Health Perspect 115:80–86.

EFSA (European Food Safety Authority). 2006. Opinion of the Scientific Panel on Food Additives, Flavourings, Processing Aids and Materials in Contact with Food on a request from the commission related to 2,2-bis(4-hydroxyphenyl) propane (bisphenol A). EFSA J 428:1–75. Available: http://www.efsa.europa.eu/EFSA/efsa_locale-1178620753812_1178620772817.htm [accessed 23 January 2009].

Environment Canada. 2008. Screening Assessment for the Challenge Phenol, 4,4'-(1-Methylethylidene)bis-(Bisphenol A), Chemical Abstracts Service Registry Number 80-05-7. Available: http://www.ec.gc.ca/substances/ese/eng/challenge/batch2/batch2_80-05-7.cfm [accessed 15 August 2008].

Food Quality Protection Act of 1996. 1996. Public Law 104-170.

Golafshani N. 2003. Understanding reliability and validity in qualitative research. Qualitative Rep 8(4):597–607.

Goldman D. 1988. Chemical aspects of compliance with Good Laboratory Practices. In: Good Laboratory Practices: An Agrochemical Perspective (Garner WY, Barge SB, eds). Washington DC: American Chemical Society, 13–23.

Gupta C. 2000. Reproductive malformation of the male offspring following maternal exposure to estrogenic chemicals. Proc Soc Exp Biol Med 224(2):61–68.

Heindel JJ, vom Saal FS. 2008. Meeting report: batch-to-batch variability in estrogenic activity in commercial animal diets—importance and approaches for laboratory animal research. Environ Health Perspect 116:389–393.

Ho SM, Tang WY, Belmonte de Frausto J, Prins GS. 2006. Developmental exposure to estradiol and bisphenol A increases susceptibility to prostate carcinogenesis and epigenetically regulates phosphodiesterase type 4 variant 4. Cancer Res 66(11):5624–5632.

Honma S, Suzuki A, Buchanan DL, Katsu Y, Watanabe H, Iguchi T. 2002. Low dose effect of in utero exposure to bisphenol A and diethylstilbestrol on female mouse reproduction. Reprod Toxicol 16:117–122.

Hugo ER, Brandebourg TD, Woo JG, Loftus J, Alexander JW, Ben-Jonathan N. 2008. Bisphenol A at environmentally relevant doses inhibits adiponectin release from human adipose tissue explants and adipocytes. Environ Health Perspect 116:1642–1647.

Institute of Laboratory Animal Research. 1996. Guide for the Care and Use of Laboratory Animals. Washington, DC:National Academy Press.

Jenkins S, Raghuraman N, Eltoum I, Carpenter M, Russo J, Lamartiniere CA. 2009. Oral Exposure to Bisphenol A Increases Dimethylbenzanthracene-Induced Mammary Cancer in Rats. Environ Health Perspect doi:10.1289/ehp.11751 [Online 7 January 2009].

Keri RA, Ho SM, Hunt PA, Knudsen KE, Soto AM, Prins GS. 2007. An evaluation of evidence for the carcinogenic activity of bisphenol A. Reprod Toxicol 24(2):240–252.

Lang IA, Galloway TS, Scarlett A, Henley WE, Depledge M, Wallace RB, et al. 2008. Association of urinary bisphenol A concentration with medical disorders and laboratory abnormalities in adults. JAMA 300(11):1303–1310.

LaPensee EW, Tuttle TR, Fox SR, Ben-Jonathan N. 2009. Bisphenol A at low nanomolar doses confers chemoresistance in estrogen receptor-α–positive and –negative breast cancer cells. Environ Health Perspect 117:175–180.

Leranth C, Hajszan T, Szigeti-Buck K, Bober J, MacLusky NJ. 2008. Bisphenol A prevents the synaptogenic response to estradiol in hippocampus and prefrontal cortex of ovariectomized nonhuman primates. Proc Nat Acad Sci 105(37):14187–14191.

Lublin JS. 1978. Safety problems. Wall Street Journal (New York) 21 February: A1.

Markey CM, Luque EH, Munoz De Toro M, Sonnenschein C, Soto AM. 2001. In utero exposure to bisphenol A alters the development and tissue organization of the mouse mammary gland. Biol Reprod 65(4):1215–1223. [Erratum in Biol Reprod 71:1753 (2004) reported that the actual doses used were 25 and 250 ng/kg/day].

Markey CM, Wadia PR, Rubin BS, Sonnenschein C, Soto AM. 2005. Long-term effects of fetal exposure to low doses of the xenoestrogen bisphenol-A in the female mouse genital tract. Biol Reprod 72(6):1344–1351.

Markowitz GE, Rosner D. 2002. Deceit and Denial: The Deadly Politics of Industrial Revolution. Berkeley, CA:University of California Press.

Moral R, Wang R, Russo IH, Lamartiniere CA, Pereira J, Russo J. 2008. Effect of prenatal exposure to the endocrine disruptor bisphenol A on mammary gland morphology and gene expression signature. J Endocrinol 196(1):101–112.

Munoz-de-Toro M, Markey CM, Wadia PR, Luque EH, Rubin BS, Sonnenschein C, et al. 2005. Perinatal exposure to bisphenol-A alters peripubertal mammary gland development in mice. Endocrinology 146(9):4138–4147.

Murray TJ, Maffini MV, Ucci AA, Sonnenschein C, Soto AM. 2007. Induction of mammary gland ductal hyperplasias and carcinoma in situ following fetal bisphenol A exposure. Reprod Toxicol 23(3):383–390.

Nagel SC, vom Saal FS, Thayer KA, Dhar MG, Boechler M, Welshons WV. 1997. Relative binding affinity-serum modified access (RBA-SMA) assay predicts the relative *in vivo* bioactivity of the xenoestrogens bisphenol A and octylphenol. Environ Health Perspect 105:70–76.

Newbold R. 1995. Cellular and molecular effects of developmental exposure to diethylstilbestrol: implications for other environmental estrogens. Environ Health Perspect 103(suppl 7):83–87.

Newbold RR, Jefferson WN, Padilla-Banks E. 2007. Long-term adverse effects of neonatal exposure to bisphenol A on the murine female reproductive tract. Reprod Toxicol 24(2):253–258.

Nikaido Y, Yoshizawa K, Danbara N, Tsujita-Kyutoku M, Yuri T, Uehara N, et al. 2004. Effects of maternal xenoestrogen exposure on development of the reproductive tract and mammary gland in female CD-1 mouse offspring. Reprod Toxicol 18(6):803–811.

Nonneman DJ, Ganjam VK, Welshons WV, Vom Saal FS. 1992. Intrauterine position effects on steroid metabolism and steroid receptors of reproductive organs in male mice. Biol Reprod 47(5):723–729.

NTP (National Toxicology Program). 2001. National Toxicology Program's Report of the Endocrine Disruptors Low Dose Peer Review. Available: http://ntp.niehs.nih.gov/ntp/htdocs/liason/LowDosePeerFinalRpt.pdf [accessed 23 January 2009].

NTP (National Toxicology Program). 2008. NTP-CERHR Monograph on the Potential Human Reproductive and Developmental Effects of Bisphenol A. Available: http://cerhr.niehs.nih.gov/chemicals/bisphenol/bisphenol.pdf [accessed 28 January 2009].

Ogura Y, Ishii K, Kanda H, Kanai M, Arima K, Wang Y, et al. 2007. Bisphenol A induces permanent squamous change in mouse prostatic epithelium. Differentiation 75(8):745–756.

Putz O, Schwartz CB, Kim S, LeBlanc GA, Cooper RL, Prins GS. 2001. Neonatal low-and high-dose exposure to estradiol benzoate in the male rat: 1. Effects on the prostate gland. Biol Reprod 65:1496–1505.

Richter CA, Birnbaum LS, Farabollini F, Newbold RR, Rubin BS, Talsness CE, et al. 2007a. In vivo effects of bisphenol A in laboratory rodent studies. Reprod Toxicol 24(2):199–224.

Richter CA, Taylor JA, Ruhlen RR, Welshons WV, vom Saal FS. 2007b. Estradiol and bisphenol A stimulate androgen receptor and estrogen receptor gene expression in fetal mouse prostate cells. Environ Health Perspect 115:902–908.

Ropero AB, Alonso-Magdalena P, Garcia-Garcia E, Ripoll C, Fuentes E, Nadal A. 2008. Bisphenol-A disruption of the endocrine pancreas and blood glucose homeostasis. Int J Androl 31(2):194–200.

Ruhlen RL, Howdeshell, KL, Mao J, Taylor JA, Bronson FH, Newbold RR, et al. 2008. Low phytoestrogen levels in feed increase fetal serum estradiol resulting in the "fetal estrogenization syndrome" and obesity in CD-1 mice. Environ Health Perspect 116:322–328.

Sheehan DM. 2000. Activity of environmentally relevant low doses of endocrine disruptors and the bisphenol A controversy: initial results confirmed. Proc Soc Exp Biol Med 224(2):57–60.

Soto AM, Vandenberg LN, Maffini MV, Sonnenschein C. 2008. Does breast cancer start in the womb? Basic Clin Pharmacol Toxicol 102(2):125–133.

Susiarjo M, Hassold TJ, Freeman E, Hunt PA. 2007. Bisphenol A exposure in utero disrupts early oogenesis in the mouse. PLoS Genet 3(1):63–70.

Thayer KA, Ruhlen RL, Howdeshell KL, Buchanan DL, Cooke PS, Preziosi D, et al. 2001. Altered prostate growth and daily sperm production in male mice exposed prenatally to subclinical doses of 17alpha-ethinyl oestradiol. 16(5):988–996.

Thigpen JE, Haseman JK, Saunders HE, Setchell KDR, Grant MG, Forsythe DB. 2003. Dietary phytoestrogens accelerate the time of vaginal opening in immature CD-1 mice. Comp Med 53:477–485.

Timms BG, Howdeshell KL, Barton L, Bradley S, Richter CA, vom Saal FS. 2005. Estrogenic chemicals in plastic and oral contraceptives disrupt development of the mouse prostate and urethra. Proc Natl Acad Sci U S A 102:7014–7019.

Triendl R. 2001. Genes may solve hormone-disrupter debate. Nature 409:274.

Tyl RW, Myers C, Marr M, Sloan CS, Castillo N, Veselica MM, et al. 2008a. Two-generation reproductive toxicity study of dietary bisphenol A (BPA) in CD-1 (Swiss) mice. Toxicol Sci 104:362–384.

Tyl R, Myers C, Marr M, Sloan CS, Castillo N, Veselica MM, et al. 2008b. Two-generation reproductive toxicity evaluation of dietary 17β-estradiol (E2; CAS No. 50-28-2) in CD-1 (Swiss) mice. Toxicol Sci 102(2):392–412.

Tyl RW, Myers CB, Marr MC, Thomas BF, Keimowitz AR, Brine DR, et al. 2002. Three-generation reproductive toxicity study of dietary bisphenol A in CD Sprague-Dawley rats. Toxicol Sci 68(1):121–146.

U.S. EPA. 2008. Good Laboratory Practices Standards. Available: http://www.epa.gov/Compliance/monitoring/programs/fifra/glp.html [accessed 15 August 2007].

U.S. FDA. 2008a. Draft assessment of bisphenol A for use in food contact applications. Available: http://www.fda.gov/ohrms/dockets/ac/08/briefing/2008-0038b1_01_02_FDA%20BPA%20Draft%20Assessment.pdf [accessed 14 August 2008].

U.S. FDA. 2008b. Statement of Norris Alderson, Ph.D., Associate Commissioner for Science, Food and Drug Administration, Department of Health and Human Services, before the Subcommittee on Commerce, Trade and Consumer Protection, Committee on Energy and Commerce. U.S. House of Representatives. June 10, 2008. Available: http://www.fda.gov/ola/2008/BPA061008.html [accessed 23 January 2009].

Vandenberg LN, Hauser R, Marcus M, Olea N, Welshons WV. 2007a. Human exposure to bisphenol A (BPA). Reprod Toxicol 24(2):139–177.

Vandenberg LN, Maffini MV, Wadia PR, Sonnenschein C, Rubin BS, Soto AM. 2007b. Exposure to environmentally relevant doses of the xenoestrogen bisphenol-A alters development of the fetal mouse mammary gland. Endocrinology 148(1):116–127.

Vandenberg LN, Wadia PR, Schaeberle CM, Rubin BS, Sonnenschein C, Soto AM. 2006. The mammary gland response to estradiol: monotonic at the cellular level, non-monotonic at the tissue-level of organization? J Steroid Biochem Mol Biol 101(4–5):263–274.

vom Saal FS. 2008. Bisphenol A: update of current published studies. Available: http://endocrinedisruptors.missouri.edu/vomsaal/vomsaal.html [accessed 31 July 2008].

vom Saal FS, Akingbemi BT, Belcher SM, Birnbaum LS, Crain DA, Eriksen M, et al. 2007. Chapel Hill bisphenol A expert panel consensus statement: integration of mechanisms, effects in animals and potential to impact human health at current levels of exposure. Reprod Toxicol 24(2):131–138.

vom Saal FS, Cooke PS, Buchanan DL, Palanza P, Thayer KA, Nagel SC, et al. 1998. A physiologically based approach to the study of bisphenol A and other estrogenic chemicals on the size of reproductive organs, daily sperm production, and behavior. Toxicol Ind Health 14(1–2):239–260.

vom Saal FS, Hughes C. 2005. An extensive new literature concerning low-dose effects of bisphenol A shows the need for a new risk assessment. Environ Health Perspect 113:926–933.

vom Saal FS, Timms BG, Montano MM, Palanza P, Thayer KA, Nagel SC, et al. 1997. Prostate enlargement in mice due to fetal exposure to low doses of estradiol or diethylstilbestrol and opposite effects at high doses. Proc Nat Acad Sci USA 94(5):2056–2061.

vom Saal FS, Welshons WV. 2006. Large effects from small exposures. II. The importance of positive controls in low-dose research on bisphenol A. Environ Res 100:50–76.

Wadia PR, Vandenberg LN, Schaeberle CM, Rubin BS, Sonnenschein C, Soto AM. 2007. Perinatal bisphenol A exposure increases estrogen sensitivity of the mammary gland in diverse mouse strains. Environ Health Perspect 115:592–598.

Welshons WV, Nagel SC, vom Saal FS. 2006. Large effects from small exposures. III. Endocrine mechanisms mediating effects of bisphenol A at levels of human exposure. Endocrinology 147(suppl 6):S56–S69.

Wetherill YB, Akingbemi BT, Kanno J, McLachlan JA, Nadal A, Sonnenschein C, et al. 2007. In vitro molecular mechanisms of bisphenol A action. Reprod Toxicol 24(2):178–198.

Wozniak AL, Bulayeva NN, Watson CS. 2005. Xenoestrogens at picomolar to nanomolar concentrations trigger membrane estrogen receptor-alpha-mediated Ca^{2+} fluxes and prolactin release in GH3/B6 pituitary tumor cells. Environ Health Perspect 113:431–439.

Zsarnovszky A, Le HH, Wang HS, Belcher SM. 2005. Ontogeny of rapid estrogen-mediated extracellular signal-regulated kinase signaling in the rat cerebellar cortex: potent nongenomic agonist and endocrine disrupting activity of the xenoestrogen bisphenol A. Endocrinology 146(12):5388–5396.

Neuroscience 155 (2008) 780–788

IDENTIFICATION OF GENES THAT RESTRICT ASTROCYTE DIFFERENTIATION OF MIDGESTATIONAL NEURAL PRECURSOR CELLS

T. SANOSAKA,[a] M. NAMIHIRA,[a] H. ASANO,[a] J. KOHYAMA,[a] K. AISAKI,[b] K. IGARASHI,[b] J. KANNO[b] AND K. NAKASHIMA[a]*

[a]*Laboratory of Molecular Neuroscience, Graduate School of Biological Sciences, Nara Institute of Science and Technology, 8916-5, Takayama, Ikoma, Nara 630-0101, Japan*

[b]*Division of Cellular and Molecular Toxicology, Biological Safety Research Center, National Institutes of Health Sciences, 1-18-1, Kamiyoga, Setagaya-ku, Tokyo 158-8501, Japan*

Abstract—During development of the mammalian CNS, neurons and glial cells (astrocytes and oligodendrocytes) are generated from common neural precursor cells (NPCs). However, neurogenesis precedes gliogenesis, which normally commences at later stages of fetal telencephalic development. Astrocyte differentiation of mouse NPCs at embryonic day (E) 14.5 (relatively late gestation) is induced by activation of the transcription factor signal transducer and activator of transcription (STAT) 3, whereas at E11.5 (mid-gestation) NPCs do not differentiate into astrocytes even when stimulated by STAT3-activating cytokines such as leukemia inhibitory factor (LIF). This can be explained in part by the fact that astrocyte-specific gene promoters are highly methylated in NPCs at E11.5, but other mechanisms are also likely to play a role. We therefore sought to identify genes involved in the inhibition of astrocyte differentiation of NPCs at midgestation. We first examined gene expression profiles in E11.5 and E14.5 NPCs, using Affymetrix GeneChip analysis, applying the Percellome method to normalize gene expression level. We then conducted *in situ* hybridization analysis for selected genes found to be highly expressed in NPCs at midgestation. Among these genes, we found that *N-myc* and high mobility group AT-hook 2 (*Hmga2*) were highly expressed in the E11.5 but not the E14.5 ventricular zone of mouse brain, where NPCs reside. Transduction of *N-myc* and *Hmga2* by retroviruses into E14.5 NPCs, which normally differentiate into astrocytes in response to LIF, resulted in suppression of astrocyte differentiation. However, sustained expression of *N-myc* and *Hmga2* in E11.5 NPCs failed to maintain the hypermethylated status of an astrocyte-specific gene promoter. Taken together, our data suggest that astrocyte differentiation of NPCs is regulated not only by DNA methylation but also by genes whose expression is controlled spatio-temporally during brain development.

*Corresponding author. Tel: +81-743-72-5471; fax: +81-743-72-5479.
E-mail address: kin@bs.naist.jp (K. Nakashima).

Abbreviations: bHLH, basic helix–loop–helix; BMP, bone morphogenetic protein; CNTF, ciliary neurotrophic factor; CT-1, cardiotrophin-1; DIG, digoxigenin; E, embryonic day; Gapdh, glyceraldehyde-3-phosphate dehydrogenase; GEO, Gene Expression Omnibus; *gfap*, glial fibrillary acidic protein; *Hmga2*, high mobility group AT-hook 2; JAK, janus kinase; LIF, leukemia inhibitory factor; NPC, neural precursor cell; SSC, sodium chloride sodium citrate; STAT, signal transducer and activator of transcription.

Key words: *N-myc*, *Hmga2*, epigenetics, Percellome method, differentiation.

The mammalian CNS is composed of neurons, astrocytes, and oligodendrocytes. Although these three cell types are derived from common multipotent neural precursor cells (NPCs), their differentiation is spatially and temporally regulated during development (Temple, 2001). Fetal telencephalic NPCs divide symmetrically in early gestation to increase their own numbers, and then undergo neurogenesis through mostly asymmetric divisions. Toward the end of the neurogenic phase, NPCs acquire multipotentiality to generate astrocytes and oligodendrocytes as well as neurons. It has recently become apparent that NPC fate determination is controlled by both extracellular cues, including cytokine signaling, and intracellular programs such as epigenetic gene regulation (Edlund and Jessell, 1999; Takizawa et al., 2001; Hsieh and Gage, 2004).

Interleukin (IL) -6 family cytokines such as cardiotrophin-1 (CT-1), leukemia inhibitory factor (LIF) and ciliary neurotrophic factor (CNTF) activate the janus kinase (JAK) –signal transducer and activator of transcription (STAT) signaling pathway and are known to induce astrocyte differentiation of NPCs (Bonni et al., 1997; Rajan and McKay, 1998). Gene knockouts of LIF (Bugga et al., 1998), LIF receptor β (Koblar et al., 1998), the common receptor component gp130 (Nakashima et al., 1999a) and STAT3 (He et al., 2005) all result in impaired astrocyte differentiation *in vivo*, emphasizing the contribution of JAK-STAT signaling to astrogliogenesis in the developing CNS. Bone morphogenetic proteins (BMPs) are another group of astrocyte-inducing cytokines. They synergistically induce astrocytic differentiation of NPCs via formation of a complex between STATs and BMP-activated transcription factor Smads, bridged by the transcriptional coactivators p300/CBP (Nakashima et al., 1999b).

In addition to these extracellular factors, intracellular programs and factors also play critical roles to regulate astrocytic differentiation of NPCs. We have previously shown that a CpG dinucleotide within a STAT3-binding element (TTC*CG*AGAA) in the astrocytic marker glial fibrillary acidic protein (*gfap*) gene promoter is highly methylated in NPCs at midgestation (embryonic day (E)11.5), when the cells differentiate only into neurons but not into astrocytes. Since STAT3 does not bind to the methylated cognate sequence, NPCs at midgestation do not express *gfap* even when stimulated by STAT3-activating cytokines such as LIF. As gestation proceeds, the STAT3-binding

0306-4522/08$32.00+0.00
doi:10.1016/j.neuroscience.2008.06.039

site becomes gradually demethylated in NPCs, enabling them to express *gfap* in response to LIF stimulation (**Takizawa et al., 2001**). Thus, we have proposed that DNA methylation is a critical cell-intrinsic determinant of astrocyte differentiation during brain development. However, the important question of how this astrocyte-specific gene promoter becomes demethylated in NPCs remains unanswered.

Neurogenic basic helix–loop–helix (bHLH) transcription factors have been also shown to regulate astrocyte differentiation during early neural development. Mice carrying mutations in *mash1* and *math3* (**Tomita et al., 2000**), or, to a lesser extent, *mash1* and *ngn2* (**Nieto et al., 2001**) exhibit decreased neurogenesis and premature astrogliogenesis. Conversely, overexpression of neurogenic bHLH factors, either *in vivo* during the gliogenic period (**Cai et al., 2000**) or in cultured NPCs exposed to CNTF (**Sun et al., 2001**), promotes neurogenesis at the expense of astrogliogenesis. A possible mechanism underlying the repressive effect on astrogliogenesis is that Ngn1 binds to p300/CBP and sequesters them away from STAT3, thereby preventing STAT3 from activating astrocytic gene expression (**Sun et al., 2001**). Such a mechanism may ensure the restriction of astrocyte differentiation in NPCs that would otherwise differentiate into neurons under the influence of high-level neurogenic bHLH factor expression during the neurogenic period.

Although these studies have provided us with an integrated insight into the mechanism of neurogenic-to-gliogenic switching in NPCs, they do not preclude the involvement of other, as yet unknown, factors. To identify such factors, we first in this study examined gene expression profiles of mid- and late-gestational NPCs by Affymetrix GeneChip analysis, which is widely used to obtain a complete picture of developmental stage-specific gene expression (**Abramova et al., 2005**; **Ajioka et al., 2006**). We then performed *in situ* hybridization experiments to investigate the spatio-temporal expression pattern of genes that were found to be highly expressed in midgestational NPCs. Two genes, *N-myc* and high mobility group AT-hook 2 (*Hmga2*), were highly expressed in the ventricular zone of E11.5 but not of E14.5 mouse brain. Transduction of *N-myc* and *Hmga2* into E14.5 NPCs resulted in suppression of astrocyte differentiation, even in the presence of LIF. However, the prolonged expression of these genes in E11.5 NPCs failed to preserve the hypermethylated status of the astrocyte-specific *gfap* promoter. These results suggest that the inhibition of astrocyte differentiation in midgestational NPCs is regulated not only by DNA methylation of astrocyte-specific gene promoters but also by transcription-regulating factors whose expression is controlled spatiotemporally during brain development.

EXPERIMENTAL PROCEDURES

NPC culture

Timed-pregnant ICR mice were used to prepare NPCs. The protocols described below were carried out according to the animal experimentation guidelines of Nara Instititute of Science and Technology that comply with National Institutes of Health Guide for Care and Use of Laboratory Animals. All efforts were made to minimize the number of animals used and their suffering. NPCs were prepared from telencephalons of E11.5 and E14.5 mice and cultured as described previously (**Nakashima et al., 1999b**). Briefly, the telencephalons were triturated in Hanks' balanced salt solution by mild pipetting with a 1-ml pipet tip (Gilson, Middleton, WI, USA). Dissociated cells were cultured in N2-supplemented Dulbecco's Modified Eagle's Medium with F12 (GIBCO, Grand Island, NY, USA) containing 10 ng/ml basic FGF (R&D Systems, Minneapolis, MN, USA) (N2/DMEM/F12/bFGF) on culture dishes (Nunc, Naperville, IL, USA) or chamber slides (Nunc) which had been precoated with poly-L-ornithine (Sigma, St. Louis, MO, USA) and fibronectin (Sigma).

Immunocytochemistry

E11.5 and E14.5 NPCs cultured on coated chamber slides were washed with PBS, fixed in 4% paraformaldehyde in PBS, and stained with the following primary antibodies: rabbit anti-SOX2 (1:1000, Chemicon, Temecula, CA, USA), mouse anti-βIII-tubulin (1:500, Sigma), rabbit anti-GFAP (1:2000, Dako, High Wycombe, UK). The following secondary antibodies were used: Alexa488-conjugated goat anti-rabbit IgG (1:500, Molecular Probes, Eugene, OR, USA), Cy3-conjugated goat anti-mouse IgG (1:500, Chemicon). Nuclei were stained using bisbenzimide H33258 fluorochrome trihydrochloride (Nacalai Tesque, Kyoto, Japan). All experiments were independently replicated at least three times.

Sample preparation and GeneChip analysis

These procedures were conducted according to the Percellome method (**Kanno et al., 2006**) to normalize mRNA expression values to sample cell numbers by adding external spike mRNAs to the sample in proportion to the genomic DNA concentration and utilizing the spike RNA quantity data as a dose-response standard curve for each sample. Cells cultured on coated dishes were washed with PBS, lysed in 500 ml of RLT buffer (Qiagen K.K., Tokyo, Japan) and transferred to a 1.5-ml tube. Two separate 10-μl aliquots were treated with DNAse-free RNase A (Nippon Gene, Tokyo, Japan) for 30 min at 37 °C, followed by proteinase K (Roche Diagnostics, Mannheim, Germany) for 3 h at 55 °C, and then transferred to a 96-well black plate. PicoGreen fluorescent dye (Molecular Probes) was added to each well, and then incubated for 2 min at 30 °C. The DNA concentration was measured using a 96-well fluorescence plate reader with excitation at 485 nm and emission at 538 nm. Lamda phage DNA (PicoGreen kit, Molecular Probes) was used as standard. The appropriate amount of spike RNA cocktail was added to the sample homogenates in proportion to their DNA concentration. Five independent *Bacillus subtilis* poly-A RNAs were included in the grade-dosed spike cocktail. Total RNAs were purified using an RNeasy Mini kit (Qiagen), according to the manufacturer's instructions. First-strand cDNAs were synthesized by incubating 5 μg of total RNA with 200 U SuperScript II reverse transcriptase (Invitrogen, Carlsbad, CA, USA) and 100 pmol T7-$(dT)_{24}$ primer [5′-GGCCAGTGAATTGTAATACGACTCACTATAGGGAGGCGG-$(dT)_{24}$-3′]. After second-strand synthesis, the double-stranded cDNAs were purified using a GeneChip Sample Cleanup Module (Affymetrix, Washington, DC, USA), according to the manufacturer's instructions, and labeled by *in vitro* transcription using a BioArray HighYield RNA transcript labeling kit (Enzo Life Sciences, Farmingdale, NY, USA). The labeled cRNA was then purified using a GeneChip Sample Cleanup Module (Affymetrix) and treated with fragmentation buffer at 94 °C for 35 min. For hybridization to a GeneChip Mouse Genome 430 2.0 Array (Affymetrix), 15 μg of fragmented cRNA probe was incubated with 50 pM control oligonucleotide B2, 1× eukaryotic hybridization control (1.5 pM BioB, 5 pM BioC, 25 pM BioD and 100 pM Cre), 0.1 mg/ml herring sperm

DNA, 0.5 mg/ml acetylated BSA and 1× manufacturer-recommended hybridization buffer in a 45 °C rotisserie oven for 16 h. Washing and staining were performed in a GeneChip Fluidics Station (Affymetrix) using the appropriate antibody amplification, washing and staining protocols. The phycoerythrin-stained arrays were scanned as digital image files, which were analyzed with GeneChip Operating Software (Affymetrix). The expression data were converted to copy numbers of mRNA per cell by the Percellome method, quality controlled, and analyzed using Percellome software (Kanno et al., 2006). The GeneChip data have been deposited in the NCBI Gene Expression Omnibus (GEO; http://www.ncbi.nlm.nih.gov/geo/) and is accessible through GEO series accession number GSE 10796.

Quantitative real-time RT-PCR

Quantitative real-time PCR was performed to confirm the results of GeneChip analysis. RNAs from E11.5 and E14.5 NPCs were reverse transcribed using Superscript II (Invitrogen) and amplified by PCR, with a specific pair of primers for each gene, using the Mx3000P system (Stratagene, La Jolla, CA, USA). The expression of target genes was normalized to that of glyceraldehyde-3-phosphate dehydrogenase (*Gapdh*). The gene-specific primers were as follows: mouse N-myc: N-myc-S, 5′-aactatgctgcaccctcacc-3′; N-myc-AS, 5′-tagcaagtccgagcgtgttc-3′; mouse Hmga2: Hmga2-S, 5′-ggcagccgtccacatcag-3′; Hmga2-AS, 5′-taatcctcctctgcggactc-3′; mouse Sox11: Sox11-S, 5′-gagcctgtacgacgaagtgc-3′; Sox11-AS, 5′-tgaacaccaggtcggagaag-3′; mouse Bhlhb5: Bhlhb5-S, 5′-gttgcgcctcaacatcaac-3′; Bhlhb5-AS, 5′-actttgcagaggctggac-3′; mouse Bcl11a: Bcl11a-S, 5′-gcatcaagctggagaaggag-3′; Bcl11a-AS, 5′-gagcttccatccgaaaactg-3′; mouse Gapdh: Gapdh-S, 5′-accacagtccatgccatcac-3′; Gapdh-AS, 5′-tccaccaccctgttgctgta-3′.

In situ hybridization

Digoxigenin- (DIG; Roche) labeled cRNA probes were synthesized for each gene, following the manufacturer's instructions. Cryosections were washed with PBS and fixed with 4% PFA. After fixation, sections were incubated in prehybridization solution (5× sodium chloride sodium citrate (SSC), 1% SDS, 50 μg/ml yeast transfer RNA, 50 μg/ml heparin in 50% formamide) at 70 °C for 1 h and hybridized with 500 ng/ml of DIG-labeled cRNA probes at 65 °C for 16 h. After three washes with wash solution 1 (5× SSC, 1% SDS in 50% formamide) and wash solution 3 (2× SSC in 50% formamide), sections were blocked with 10% normal sheep serum in TBST at room temperature for 1 h and then incubated with 1:1000 alkaline phosphatase-conjugated anti-DIG antibody (Roche) at 4 °C for 16 h. After four washes with TBST, hybridized probes were visualized with 5-bromo-4-chloro-3 indolylphosphate and nitro blue tetrazolium chloride.

Recombinant retrovirus construction and infection

Human *N-myc* and mouse *Hmga2* cDNAs were cloned into the expression vector pMYs, which contains an internal ribosome entry site followed by the region upstream of the *EGFP* gene (Morita et al., 2000). The Plat-E packaging cell line was transiently transfected with the retrovirus DNA by Trans-IT 293 (Mirus, Madison, WI, USA) (Morita et al., 2000). On the following day, the medium was replaced with N2/DMEM/F12/bFGF, and the cells were cultured in this medium for 1 day before virus was collected.

Fluorescence activated cell sorting

Virus-infected E11.5 NPCs were cultured for 4 days, after which GFP-labeled cells were sorted using a FACS Vantage (Becton Dickinson, Franklin Lakes, NJ, USA) at a flow rate of less than 1500 events/s; gating parameters were set by side and forward scatter to eliminate debris, dead and aggregated cells. After sorting, genomic DNA was extracted and used for bisulfite sequencing.

Bisulfite sequencing

Sodium bisulfite treatment of genomic DNA was performed using a Methylamp DNA Modification kit (Epigentek, Brooklyn, NY, USA), according to the manufacturer's instructions. The region in the *gfap* promoter containing the STAT-binding site of the bisulfite-treated genomic DNA was amplified by PCR using the following primers: GFmS (5′-GGGATTTATTAGGAGAATTTTAGAAGTAG-3′), GFmAS (5′-TCTACCCATACTTAAACTTCTAATATCTAC-3′). The PCR products were cloned into pT7Blue vector (Novagen, Madison, WI, USA) and at least 12 randomly selected clones were sequenced.

RESULTS

Preparation of NPCs from different developmental stages and comparison of their gene expression profiles by GeneChip analysis

E11.5 NPCs do not differentiate into astrocytes, even in the presence of the astrocyte-inducing cytokine LIF, in contrast to 4-day cultured E14.5 NPCs (Takizawa et al., 2001). As a first step toward identifying factors involved in the inhibition of astrocyte differentiation of NPCs at midgestation, we examined the gene expression profiles of E11.5 and E14.5 NPCs.

E11.5 and E14.5 NPCs were isolated from embryonic telencephalon and cultured as indicated in Fig. 1A. To evaluate the purity of NPCs in each cell population, the cells were stained with antibody against SOX2, an NPC marker (Graham et al., 2003). As shown in Fig. 1B and C, the majority of cells in both populations were positive for SOX2, indicating that NPCs were highly enriched. An Affymetrix mouse genome GeneChip array was chosen to compare expression profiles in the two populations, and we adopted the Percellome method to normalize gene expression from different samples (Kanno et al., 2006). The method enabled us to quantify mRNA molecules per cell based on the measurement of cell by adding a grade-dosed spike cocktail to the samples. We excluded genes whose transcript copy number was below six per cell. Scatter plots illustrating the differences between E11.5 and E14.5 NPCs are shown in Fig. 1D; 194 genes were expressed at >fivefold higher level in E11.5 NPCs than in E14.5 NPCs (Fig. 1D, light blue zone). Of these, 102 were known genes, and were classified by functional category (Fig. 1E). Since we wished to identify negative regulators of astrocyte differentiation, or factors involved in the epigenetic modification in midgestational NPCs, we focused on transcription-related genes (Fig. 1E, red). These 21 genes are listed in Table 1, and five (*N-myc*, *Hmga2*, *Bhlhb5*, *Sox11*, *Bcl11a*) were selected for further analysis because they have been reported to play roles in cell growth, differentiation, and chromatin remodeling in other types of stem cells (Sawai et al., 1990; Zhou et al., 1995; Saiki et al., 2000; Knoepfler et al., 2002; Brunelli et al., 2003; Sock et al., 2004).

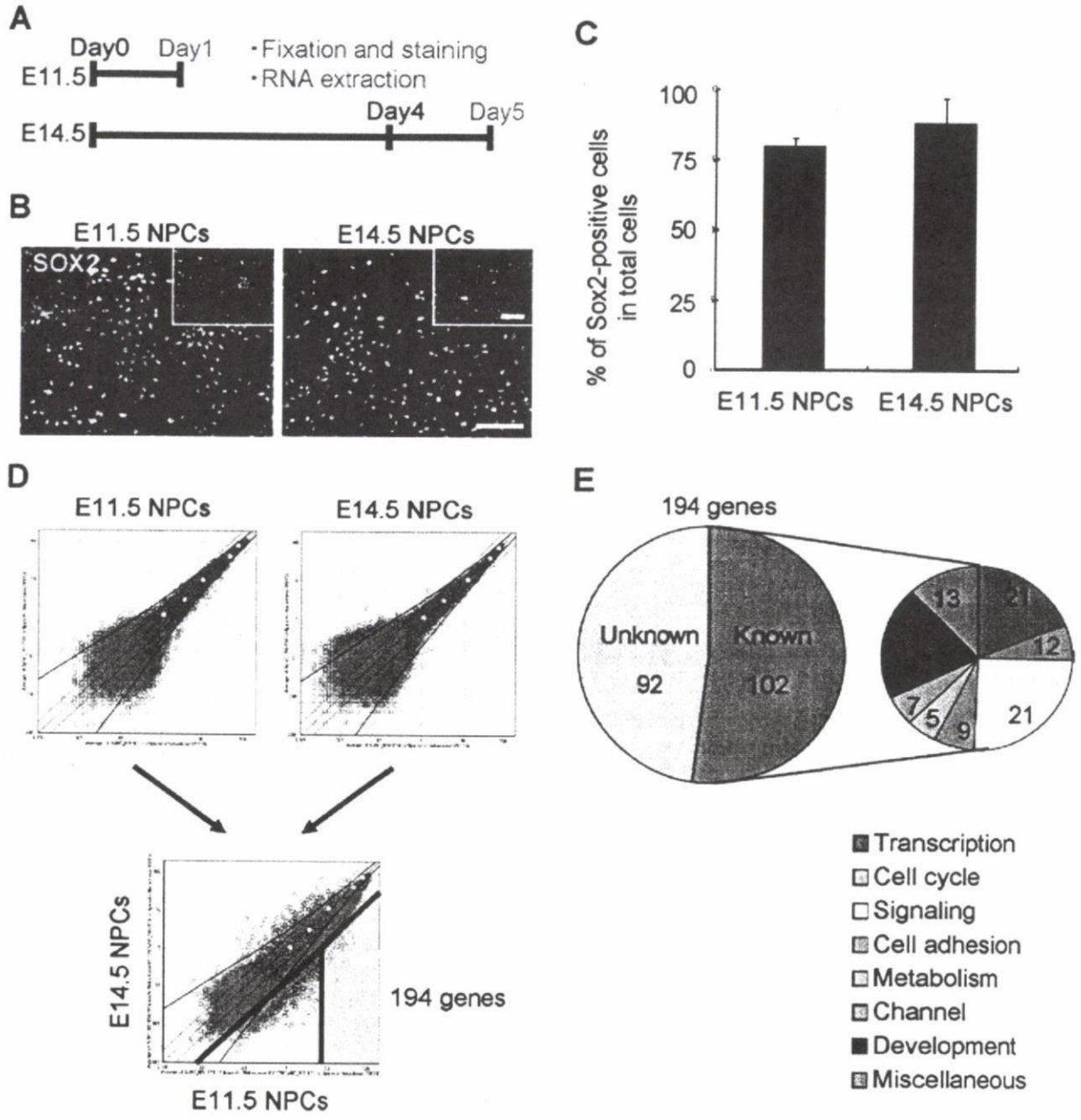

Fig. 1. Comparison of gene expression profiles in E11.5 and E14.5 NPCs. (A) Schematic of experimental protocol. NPCs isolated from E11.5 mouse telencephalon were plated (day 0) and used on the following day for immunostaining and RNA extraction (day 1). NPCs isolated at E14.5 were expanded for 4 days and replated on day 4. On day 5, these cells were fixed for immunostaining. RNA was also extracted. (B) E11.5 and E14.5 NPCs were stained with antibody against Sox2 (green). Scale bar=25 μm. Insets: Hoechst nuclear staining of each field. Scale bar=25 μm. (C) The percentage of Sox2-positive cells in E11.5 and E14.5 NPCs was quantified. Mean±S.D. (D) Scatter plots of E11.5 (upper left) and E14.5 (upper right) samples obtained from GeneChip analysis indicated no significant change between independent experiments with the same sample. Overview (lower plot) of gene expression change was compared between each sample. One hundred ninety-four genes were expressed at >fivefold higher level in E11.5 NPCs than E14.5 NPCs (light blue zone). (E) Of the 194 genes that were highly expressed in E11.5 NPCs, known genes were classified according to Affymetrix gene ontology. For interpretation of the references to color in this figure legend, the reader is referred to the Web version of this article.

Table 1. Transcription-related genes highly expressed in E11.5 NPCs

Probe set ID	GenBank ID	Gene symbol	E11.5 NPCs	E14.5 NPCs	E11.5/ E14.5
1433919_at	AV302111	*Asb4*	9.8	0.5	19.6
1419406_a_at	NM_016707	***Bcl11a***	13.8	1.8	7.7
1418271_at	NM_021560	***Bhlhb5***	10.6	1.2	8.8
1452207_at	Y15163	*Cited2*	16.7	2.6	6.4
1449470_at	NM_010053	*Dlx1*	13.8	2.4	5.8
1448877_at	NM_010054	*Dlx2*	9.8	1.8	5.4
1449863_a_at	NM_010056	*Dlx5*	11.2	0.7	16.0
1459211_at	AW546128	*Gli2*	8.0	1.5	5.3
1456067_at	AW546010	*Gli3*	20.6	2.1	9.8
1422851_at	X58380	***Hmga2***	25.5	0.5	51.0
1450723_at	BQ176915	*Ils1*	8.6	0.1	86.0
1427300_at	D49658	*Lhx8*	10.5	0.1	105.0
1417155_at	BC005453	***N-myc***	8.2	1.2	6.8
1415811_at	BB702754	*NP95*	12.6	2.1	6.0
1421193_a_at	NM_016768	*Pbx3*	12.3	1.6	7.7
1417400_at	NM_030690	*Rai14*	11.0	1.6	6.9
1435856_x_at	AV310148	*Smarcb1*	8.0	1.6	5.0
1431255_at	BB656631	***Sox11***	38.7	6.2	6.2
1450034_at	AW214029	*Stat1*	9.6	1.8	5.3
1416711_at	NM_009322	*Tbr1*	9.8	0.2	49.0
1423424_at	BB732077	*Zic3*	11.2	0.5	22.4

Genes reported to participate in cell growth, differentiation and chromatin remodeling are shown in boldface.

Spatio-temporal expression patterns of genes highly expressed in E11.5 NPCs

To substantiate the GeneChip results, we extracted RNA from E11.5 and E14.5 NPCs and performed real-time RT-PCR using specific primers for each selected gene. Consistent with the GeneChip analysis, all five genes were highly expressed in E11.5 NPCs compared with E14.5 NPCs (Fig. 2A). We next performed *in situ* hybridization for each gene using E11.5, E14.5 and E17.5 mouse brain sections (Fig. 2B). *N-myc* and *Hmga2* mRNAs were specifically detected in the ventricular zone (VZ) of E11.5 brain, implying that N-myc and Hmga2 play some role in NPCs at this stage. By contrast, *Bhlhb5*, *Sox11* and *Bcl11a* expression was stronger in cortical plate, where postmitotic neurons reside, than in the VZ (Fig. 2B). We therefore decided to analyze the function of N-myc and Hmga2 in more detail.

Transduction of *N-myc* and *Hmga2* inhibits astrocyte differentiation of E14.5 NPCs

We next examined whether N-myc and Hmga2 affect astrocyte differentiation of NPCs. We expressed EGFP alone (control), and EGFP together with either N-myc or Hmga2, using retroviral infection in E14.5 NPCs, in which expression of the endogenous genes is very low. Virus-infected E14.5 NPCs were cultured for 4 days in the presence of LIF to induce astrocyte differentiation, and then stained with antibodies against GFP and GFAP. As shown in Fig. 3A and B, NPCs infected with control virus effectively differentiated into GFAP-positive astrocytes in response to LIF stimulation (42±2.6%). In contrast, GFAP-positive astrocyte differentiation was virtually abolished in cells ectopically expressing N-myc (0.5±0.4%) and Hmga2 (3±2.0%) (Fig. 3A, B). Expression of these genes did not significantly affect neuronal differentiation of NPCs, as assessed by monitoring expression of the neuronal marker βIII-tubulin, compared with the control cells (Fig. 3C, D). We further examined whether the observed suppression of astrocyte differentiation of NPCs infected with viruses encoding N-myc or Hmga2 could be attributed to specific cell-growth inhibition or to cell death. To address this issue, we performed immune staining for the cycling cell marker Ki67 and the apoptotic marker cleaved caspase 3. Although proliferation of NPCs ectopically expressing N-myc or Hmga2 appeared to be slightly enhanced, expression of either gene caused negligible cell death. These results suggest that N-myc and Hmga2 inhibit astrocyte differentiation of NPCs by a mechanism distinct from that of the neurogenic bHLH factors, which enhance neuronal differentiation (Sun et al., 2001).

Continuous expression of N-myc and Hmga2 in E11.5 NPCs fails to preserve the hypermethylated status of an astrocyte-specific gene promoter

We have previously shown that the *gfap* promoter is highly methylated in E11.5 NPCs, and becomes demethylated as gestation proceeds (Takizawa et al., 2001). This demethylation enables NPCs at later developmental stages, E14.5 or thereafter, to respond to LIF and differentiate into GFAP-positive astrocytes. As shown in the foregoing data, expression levels of *N-myc* and *Hmga2* thus seemed to be reduced concurrently with the developmental stage-dependent demethylation of an astrocyte-specific gene promoter; furthermore, ectopic expression of these genes in E14.5 NPCs inhibited GFAP-positive astrocyte differentiation. We therefore hypothesized that sustained expression of N-myc and Hmga2 in E11.5 NPCs might maintain the hypermethylated status of the *gfap* promoter. To test this, we infected E11.5 NPCs with viruses expressing EGFP alone and EGFP together with either N-myc or Hmga2 and cultured them for 4 days. GFP-positive cells were sorted by FACS and their genomic DNAs were extracted for bisulfite sequencing. As observed in the previous study (Takizawa et al., 2001), the *gfap* promoter including the STAT3 site became demethylated to about 65% in control virus-infected cells after the 4-day culture, and this was also the case for both N-myc- and Hmga2-expressing virus-infected cells (Fig. 3E, F). These results indicate that sustained expression of N-myc and Hmga2 in E11.5 NPCs does not affect the process of demethylation in this astrocyte-specific gene promoter. On the other hand, when 4-day-cultured control virus-infected E11.5 NPCs were then stimulated with LIF for an additional 4 days, GFAP-positive astrocytes appeared, probably due to demethylation in the promoter, whereas neither *N-myc* nor *Hmga2* virus-infected cells gave rise to astrocytes even in the presence of LIF (data not shown). These results suggest that N-myc and Hmga2 inhibit precocious astrocyte differentiation of midgestational NPCs independent of the DNA methylation status of an astrocyte-specific gene promoter.

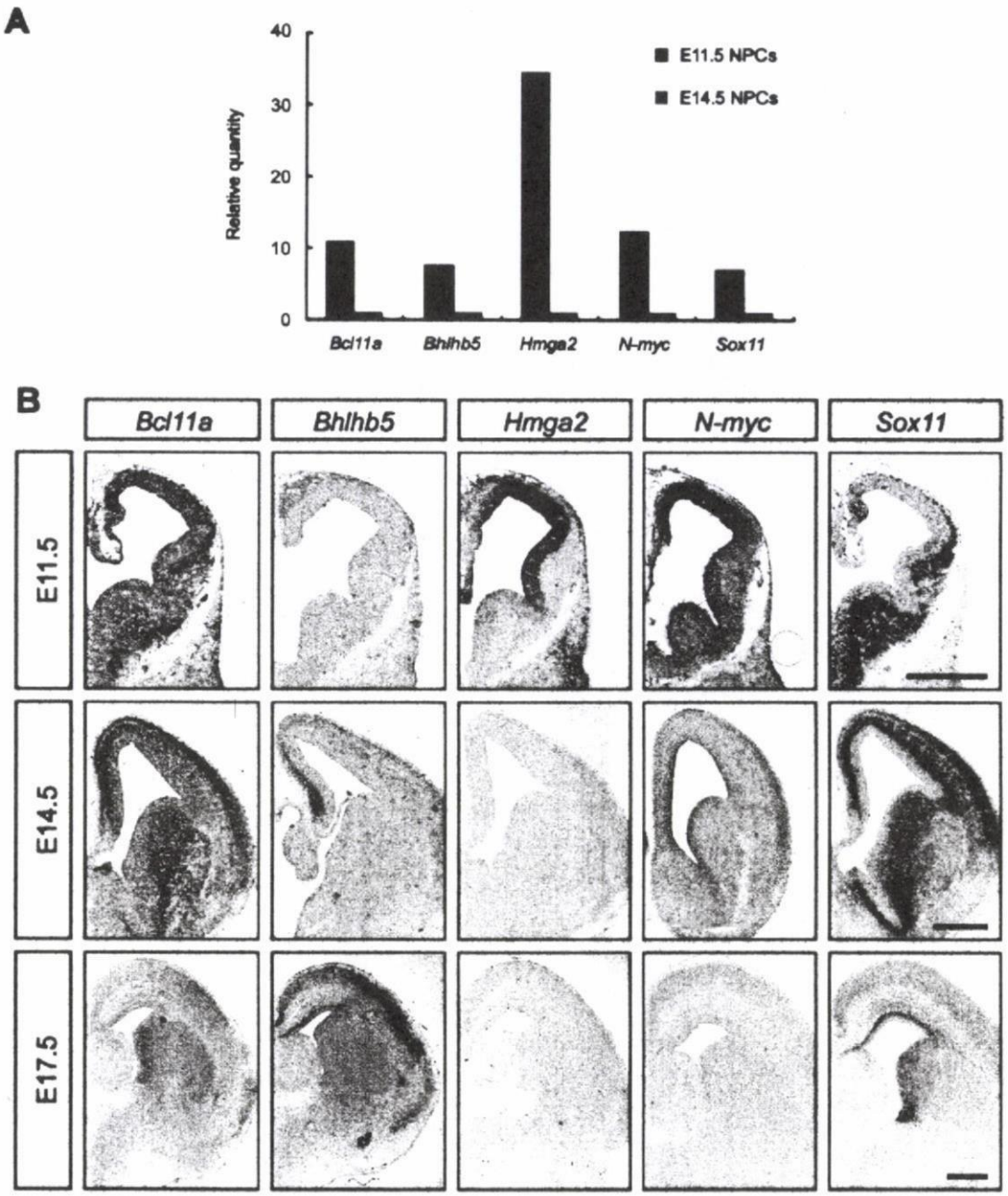

Fig. 2. *N-myc* and *Hmga2* are highly expressed in the VZ of E11.5 mouse brain. (A) Gene-specific real-time RT-PCR was performed to validate GeneChip analysis data. (B) *In situ* hybridization was performed for E11.5, E14.5 and E17.5 mouse brain sections. No signal was detected when sense-probes for each gene were used (data not shown). Scale bar=500 μm.

DISCUSSION

In this study, we compared NPC gene expression profiles at different developmental stages using Affymetrix GeneChips and the Percellome method, and then analyzed by *in situ* hybridization the spatio-temporal expression patterns of genes which were highly expressed in E11.5 NPCs. We found that *N-myc* and *Hmga2* were specifically expressed in E11.5 NPC both *in vivo* and *in vitro* and, furthermore, that the transduction of these genes into NPCs suppressed LIF-induced astrocytic differentiation without affecting DNA demethylation of the astrocyte-specific *gfap* gene promoter.

The basic HLH leucine zipper transcription factor N-myc,a member of the myc family of oncogenes, is a nuclear phosphoprotein exhibiting site-specific DNA-binding activity (Ramsay et al., 1986; Alex et al., 1992), and has

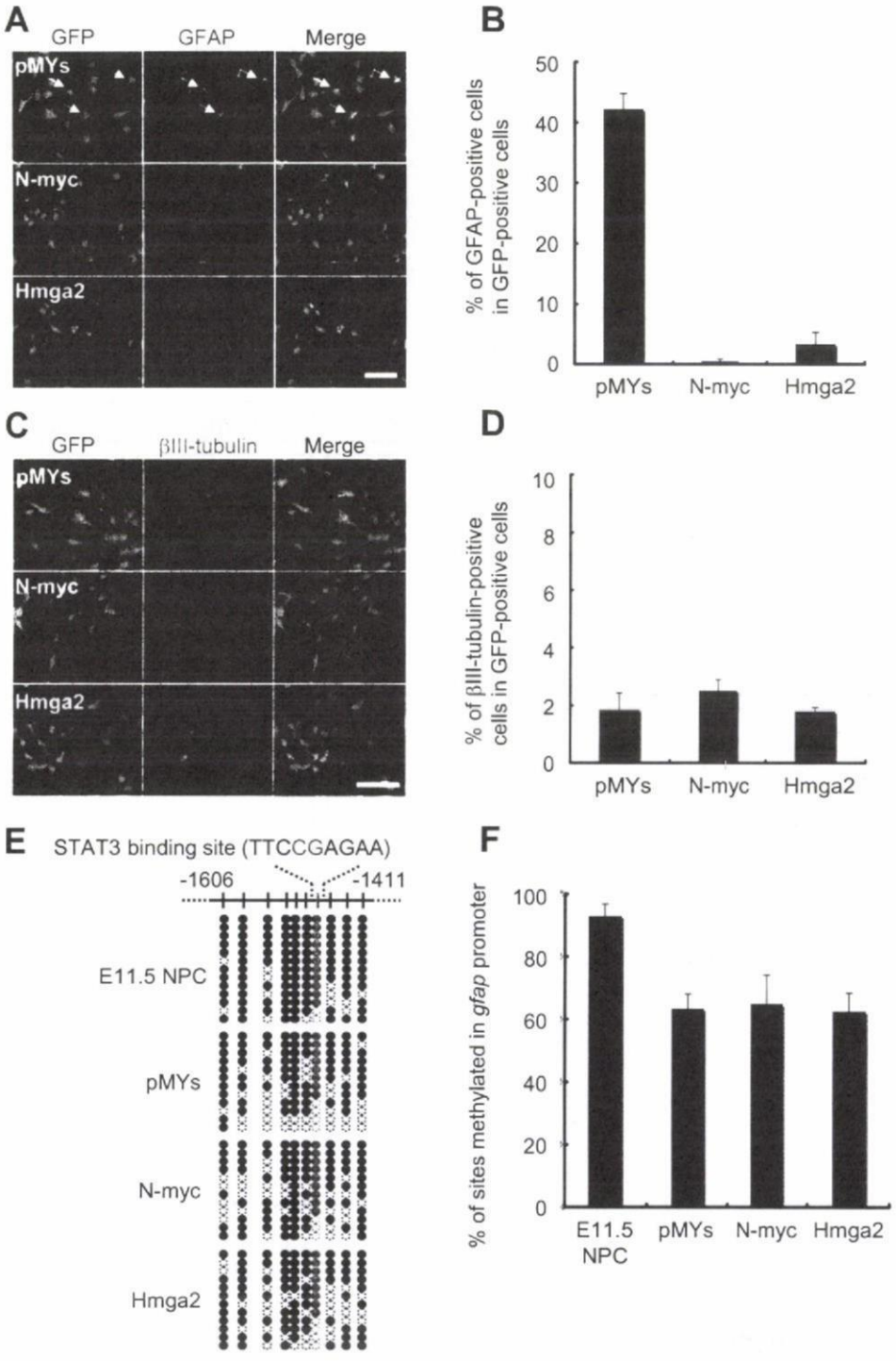

Fig. 3. N-myc and Hmga2 inhibit astrocyte differentiation of NPCs even in the presence of LIF. (A–D) E14.5 NPCs were infected with recombinant retroviruses engineered to express *EGFP* alone (pMYs), and *EGFP* together with either *N-myc* (N-myc) or *Hmga2* (Hmga2), and cultured with LIF (50 ng/ml) for 4 days to induce astrocyte differentiation. The cells were then stained with antibodies against GFP (green) and GFAP (red) (A). Arrows indicate GFP/GFAP double-positive cells. The percentage of GFAP-positive astrocytes in GFP-positive cells was quantified (B). Mean±S.D. The cells were also stained with antibodies against GFP (green) and βIII-tubulin (red) (C). The percentage of βIII-tubulin-positive neurons in GFP-positive cells was quantified (D). Mean±S.D. (E) E11.5 NPCs were infected with recombinant retroviruses engineered to express *EGFP* alone (pMYs), and *EGFP* together with either *N-myc* (N-myc) or *Hmga2* (Hmga2), and subsequently cultured for 4 days. GFP-positive cells were then sorted based on GFP fluorescence, and genomic DNA was extracted for bisulfite sequencing. White and black circles indicate unmethylated and methylated CpG sites, respectively. The E11.5 NPC sample was freshly prepared NPCs from telencephalon at E11.5. The CpG dinucleotide within the STAT3 binding site is indicated in red. (F) Methylation frequency in the *gfap* promoter. Mean±S.D. Scale bars=50 μm (A, C). For interpretation of the references to color in this figure legend, the reader is referred to the Web version of this article.

been reported to be expressed in a wide range of vertebrate tissues, primarily during embryogenesis (Schreiber-Agus et al., 1993). The mice deficient for functional *N-myc* are embryonic lethal (Stanton et al., 1992). Since N-myc has been shown to be a transcriptional activator, it may inhibit astrocyte differentiation via induction of neurogenic bHLH factors such as *Ngn1* (Sun et al., 2001), which have already been suggested to inhibit astrocyte differentiation in midgestational NPCs. However, this scenario seems unlikely because *N-myc* expression in NPCs did not affect neuronal differentiation, as assessed by monitoring expression of the neuronal marker βIII-tubulin (Fig. 3C, D). On the other hand, Hmga2 possesses an acidic C-terminal tail and three individual DNA-binding domains which bind short stretches of AT-rich DNA with high affinity (Reeves, 2001). *Hmga2* is expressed in pluripotent embryonic stem (ES) cells and in most tissues and organs during embryogenesis, but at very low levels or not at all in adult tissues (Zhou et al., 1995). Its function appears to be critical for cell growth, because mice lacking functional *Hmga2* exhibit a pygmy phenotype (Zhou et al., 1995). Recently, it was reported that Hmga2 specifically accumulates on senescent cell chromatin and that it functions as a structural component of senescence-associated heterochromatin foci and as a repressor of proliferation-associated genes (Narita et al., 2006). We therefore expected that Hmga2 would maintain the hypermethylation status of the astrocyte-specific *gfap* promoter via transcription-repressive heterochromatin formation in E11.5 NPCs. However, our results indicate that this is not the case. The mechanism(s) whereby N-myc and Hmga2 inhibit astrocyte differentiation must await further investigation.

Although DNA methylation is a critical cell-intrinsic determinant for the neurogenic-to-astrogliogenic switch and/or astrocyte differentiation of NPCs, many other spatio-temporally expressed extracellular factors such as CT-1, Notch and Wnt1 (Barnabe-Heider et al., 2005; Hirabayashi and Gotoh, 2005; Nagao et al., 2007) and intracellular factors including Ngn (Sun et al., 2001), N-CoR (Hermanson et al., 2002), N-myc and Hmga2 (this study) complement DNA methylation to ensure the sequential differentiation of NPCs during development. Thus, to better understand the mechanism underlying these processes, this study emphasizes the need to take cell-extrinsic cues, cell-intrinsic programs and factors, and their interaction into consideration.

Acknowledgments—We thank Dr. T. Kitamura (Tokyo University) for pMY vector and Plat-E cells. We appreciate Dr. Y. Bessho and T. Matsui for valuable discussions. We also thank Dr. I. Smith for helpful comments and critical reading of the manuscript. We are very grateful to N. Ueda for excellent secretarial assistance. Many thanks to N. Namihira for technical help. We also thank N. Moriyama for technical help with GeneChip analysis. This work has been supported by a Grant-in-Aid for Science Research on Priority Areas and the NAIST Global COE Program (Frontier Biosciences: Strategies for survival and adaptation in a changing global environment) from the Ministry of Education, Culture, Sports, Science and Technology (MEXT) of Japan.

REFERENCES

Abramova N, Charniga C, Goderie SK, Temple S (2005) Stage-specific changes in gene expression in acutely isolated mouse CNS progenitor cells. Dev Biol 283:269–281.

Ajioka I, Maeda T, Nakajima K (2006) Identification of ventricular-side-enriched molecules regulated in a stage-dependent manner during cerebral cortical development. Eur J Neurosci 23:296–308.

Alex R, Sozeri O, Meyer S, Dildrop R (1992) Determination of the DNA sequence recognized by the bHLH-zip domain of the N-Myc protein. Nucleic Acids Res 20:2257–2263.

Barnabe-Heider F, Wasylnka JA, Fernandes KJ, Porsche C, Sendtner M, Kaplan DR, Miller FD (2005) Evidence that embryonic neurons regulate the onset of cortical gliogenesis via cardiotrophin-1. Neuron 48:253–265.

Bonni A, Sun Y, Nadal-Vicens M, Bhatt A, Frank DA, Rozovsky I, Stahl N, Yancopoulos GD, Greenberg ME (1997) Regulation of gliogenesis in the central nervous system by the JAK-STAT signaling pathway. Science 278:477–483.

Brunelli S, Innocenzi A, Cossu G (2003) Bhlhb5 is expressed in the CNS and sensory organs during mouse embryonic development. Gene Expr Patterns 3:755–759.

Bugga L, Gadient RA, Kwan K, Stewart CL, Patterson PH (1998) Analysis of neuronal and glial phenotypes in brains of mice deficient in leukemia inhibitory factor. J Neurobiol 36:509–524.

Cai L, Morrow EM, Cepko CL (2000) Misexpression of basic helix-loop-helix genes in the murine cerebral cortex affects cell fate choices and neuronal survival. Development 127:3021–3030.

Edlund T, Jessell TM (1999) Progression from extrinsic to intrinsic signaling in cell fate specification: a view from the nervous system. Cell 96:211–224.

Graham V, Khudyakov J, Ellis P, Pevny L (2003) SOX2 functions to maintain neural progenitor identity. Neuron 39:749–765.

He F, Ge W, Martinowich K, Becker-Catania S, Coskun V, Zhu W, Wu H, Castro D, Guillemot F, Fan G, de Vellis J, Sun YE (2005) A positive autoregulatory loop of Jak-STAT signaling controls the onset of astrogliogenesis. Nat Neurosci 8:616–625.

Hermanson O, Jepsen K, Rosenfeld MG (2002) N-CoR controls differentiation of neural stem cells into astrocytes. Nature 419: 934–939.

Hirabayashi Y, Gotoh Y (2005) Stage-dependent fate determination of neural precursor cells in mouse forebrain. Neurosci Res 51: 331–336.

Hsieh J, Gage FH (2004) Epigenetic control of neural stem cell fate. Curr Opin Genet Dev 14:461–469.

Kanno J, Aisaki K, Igarashi K, Nakatsu N, Ono A, Kodama Y, Nagao T (2006) "Per cell" normalization method for mRNA measurement by quantitative PCR and microarrays. BMC Genomics 7:64.

Knoepfler PS, Cheng PF, Eisenman RN (2002) N-myc is essential during neurogenesis for the rapid expansion of progenitor cell populations and the inhibition of neuronal differentiation. Genes Dev 16:2699–2712.

Koblar SA, Turnley AM, Classon BJ, Reid KL, Ware CB, Cheema SS, Murphy M, Bartlett PF (1998) Neural precursor differentiation into astrocytes requires signaling through the leukemia inhibitory factor receptor. Proc Natl Acad Sci U S A 95:3178–3181.

Morita S, Kojima T, Kitamura T (2000) Plat-E: an efficient and stable system for transient packaging of retroviruses. Gene Ther 7: 1063–1066.

Nagao M, Sugimori M, Nakafuku M (2007) Cross talk between notch and growth factor/cytokine signaling pathways in neural stem cells. Mol Cell Biol 27:3982–3994.

Nakashima K, Wiese S, Yanagisawa M, Arakawa H, Kimura N, Hisatsune T, Yoshida K, Kishimoto T, Sendtner M, Taga T (1999a) Developmental requirement of gp130 signaling in neuronal survival and astrocyte differentiation. J Neurosci 19:5429–5434.

Nakashima K, Yanagisawa M, Arakawa H, Kimura N, Hisatsune T, Kawabata M, Miyazono K, Taga T (1999b) Synergistic signaling in

fetal brain by STAT3-Smad1 complex bridged by p300. Science 284:479–482.

Narita M, Krizhanovsky V, Nunez S, Chicas A, Hearn SA, Myers MP, Lowe SW (2006) A novel role for high-mobility group a proteins in cellular senescence and heterochromatin formation. Cell 126: 503–514.

Nieto M, Schuurmans C, Britz O, Guillemot F (2001) Neural bHLH genes control the neuronal versus glial fate decision in cortical progenitors. Neuron 29:401–413.

Rajan P, McKay RD (1998) Multiple routes to astrocytic differentiation in the CNS. J Neurosci 18:3620–3629.

Ramsay G, Stanton L, Schwab M, Bishop JM (1986) Human proto-oncogene N-myc encodes nuclear proteins that bind DNA. Mol Cell Biol 6:4450–4457.

Reeves R (2001) Molecular biology of HMGA proteins: hubs of nuclear function. Gene 277:63–81.

Saiki Y, Yamazaki Y, Yoshida M, Katoh O, Nakamura T (2000) Human EVI9, a homologue of the mouse myeloid leukemia gene, is expressed in the hematopoietic progenitors and down-regulated during myeloid differentiation of HL60 cells. Genomics 70:387–391.

Sawai S, Kato K, Wakamatsu Y, Kondoh H (1990) Organization and expression of the chicken N-myc gene. Mol Cell Biol 10:2017–2026.

Schreiber-Agus N, Horner J, Torres R, Chiu FC, DePinho RA (1993) Zebra fish myc family and max genes: differential expression and oncogenic activity throughout vertebrate evolution. Mol Cell Biol 13:2765–2775.

Sock E, Rettig SD, Enderich J, Bosl MR, Tamm ER, Wegner M (2004) Gene targeting reveals a widespread role for the high-mobility-group transcription factor Sox11 in tissue remodeling. Mol Cell Biol 24:6635–6644.

Stanton BR, Perkins AS, Tessarollo L, Sassoon DA, Parada LF (1992) Loss of N-myc function results in embryonic lethality and failure of the epithelial component of the embryo to develop. Genes Dev 6:2235–2247.

Sun Y, Nadal-Vicens M, Misono S, Lin MZ, Zubiaga A, Hua X, Fan G, Greenberg ME (2001) Neurogenin promotes neurogenesis and inhibits glial differentiation by independent mechanisms. Cell 104:365–376.

Takizawa T, Nakashima K, Namihira M, Ochiai W, Uemura A, Yanagisawa M, Fujita N, Nakao M, Taga T (2001) DNA methylation is a critical cell-intrinsic determinant of astrocyte differentiation in the fetal brain. Dev Cell 1:749–758.

Temple S (2001) The development of neural stem cells. Nature 414:112–117.

Tomita K, Moriyoshi K, Nakanishi S, Guillemot F, Kageyama R (2000) Mammalian achaete-scute and atonal homologs regulate neuronal versus glial fate determination in the central nervous system. EMBO J 19:5460–5472.

Zhou X, Benson KF, Ashar HR, Chada K (1995) Mutation responsible for the mouse pygmy phenotype in the developmentally regulated factor HMGI-C. Nature 376:771–774.

(Accepted 13 June 2008)
(Available online 21 June 2008)